Original Article

Branching patterns and variations of the bronchus and blood vessels in the superior segment of the right lower lobe: a three-dimensional computed tomographic bronchography and angiography study

Shusheng Zhu[1#], Wenzheng Xu[1#], Zhihua Li[1], Weibing Wu[1], Alessandro Brunelli[2], Yosuke Matsuura[3], Giulio Maurizi[4], Davide Tosi[5], Ilies Bouabdallah[6], Dominique Gossot[7], Liang Chen[1]

[1]Department of Thoracic Surgery, The First Affiliated Hospital of Nanjing Medical University, Nanjing, China; [2]Department of Thoracic Surgery, St. James's University Hospital, Leeds Teaching Hospitals NHS Trust, Leeds, UK; [3]Department of Thoracic Surgical Oncology, Cancer Institute Hospital, Japanese Foundation for Cancer Research, Tokyo, Japan; [4]Division of Thoracic Surgery, "Sapienza" University of Rome, "Sant'Andrea" Hospital, Rome, Italy; [5]Thoracic Surgery and Lung Transplant Unit, Fondazione IRCCS Ca' Granda Ospedale Maggiore Policlinico, Milan, Italy; [6]Department of Thoracic Surgery, Saint Joseph Hospital, Marseille, France; [7]Thoracic Department, Curie-Montsouris Thorax Institute - Institut Mutualiste Montsouris, Paris, France

Contributions: (I) Conception and design: S Zhu, L Chen; (II) Administrative support: S Zhu, L Chen; (III) Provision of study materials or patients: Z Li, W Wu, L Chen; (IV) Collection and assembly of data: S Zhu, Z Li; (V) Data analysis and interpretation: S Zhu, W Xu; (VI) Manuscript writing: All authors; (VII) Final approval of manuscript: All authors.

[#]These authors contributed equally to this work.

Correspondence to: Liang Chen, MD. Department of Thoracic Surgery, The First Affiliated Hospital of Nanjing Medical University, 300 Guangzhou Road, Nanjing 210029, China. Email: clbright0909@njmu.edu.cn.

Background: Superior segmentectomy is classified as simple due to the single intersegmental plane between the superior and basal segments. However, oncological outcomes in patients undergoing superior segmentectomy tend to be worse compared to those receiving other segmentectomy. The aim of this study is to determine the branching patterns and variations of the bronchus and blood vessels of the superior segment of the right lower lobe (RS^6).

Methods: Three-dimensional computed tomographic bronchography and angiography (3D-CTBA) was reconstructed in 316 patients who underwent enhanced chest computed tomography (CT) and subsequent surgery in our center from November 2018 to March 2021.

Results: The bronchus in RS^6 consisted of a single stem in 96.5% cases (305/316), and 2 separate stems in the remaining 3.5% cases (11/316). The artery in RS^6 consisted of a single stem in 59.5% cases (188/316), 2 separate stems in 37.0% cases (117/316), and 3 separate stems in the remaining 3.5% cases (11/316). The vein in RS^6 consisted of a single stem in 94.3% cases (298/316) and 2 separate stems in the remaining 5.7% cases (18/316). B^6 variation was noted in 1.6% cases (5/316). A^6 variation was noted in 18.0% cases (57/316), including the following: (I) coexistence of A^6 and A^2 (n=25); (II) A^6b originating from A^{9+10}/A^{10} alone (n=20); (III) A^6c originating from A^{9+10} (n=10); and (IV) co-draining of A^6 and A^7 (n=2). V^6 variation was noted in 11.7% cases (37/316), including the following: (I) co-draining of V^6 and V^2 (n=20); (II) co-draining of V^6 and V^4 (n=5); (III) V^6 and V^{8+9} co-draining (n=3); (IV) V^6 draining into the superior pulmonary vein (n=4); and (V) direct V^6 draining into the left atrium (n=5).

Conclusions: Variation of A^6 and V^6 in RS^6 is much more common than previously reported. 3D-CTBA reconstruction is useful for pre-surgery planning.

Keywords: Right lower lobe; superior segment; segmentectomy; three-dimensional computed tomographic bronchography and angiography (3D-CTBA); anatomical variations

Submitted Oct 20, 2023. Accepted for publication Dec 15, 2023. Published online Dec 26, 2023.
doi: 10.21037/jtd-23-1607
View this article at: https://dx.doi.org/10.21037/jtd-23-1607

Introduction

Segmentectomy has the benefit of conserving lung function with similar therapeutic efficacy to lobectomy for very well selected stage IA lung cancers (1-3), but is technically more challenging due to individual variation of the bronchus and blood vessels (4).

Segmentectomy could be categorized into simple versus complex based on the intersegmental plane (5). Superior segmentectomy is classified as simple due to the single intersegmental plane between the superior and basal segments. However, oncological outcomes in patients undergoing superior segmentectomy tend to be worse compared to those receiving other segmentectomy (6-8). Nakazawa *et al.* (9) reported that the issue of clipping the intersegmental plane was the cause of the right lower lobe superior segmentectomy's subpar results. The use of staplers is appropriate in the majority of cases, but may result in residual S^6 parenchyma in the cases in which the posterior portion of S^6 stretches towards the caudal direction and creates a curved intersegmental plane. Also, segmental volume and surgical margins vary depending on the anatomical landmark used for intersegmental plane identification. Surgical margins tend to be smaller when the bronchi are used instead of intersegmental veins to define the intersegmental plane (9). Considering these anatomical traits, the processing of intraoperative anatomical structures and the individualization of the intersegmental interface ultimately impacts the safety and oncology efficacy of surgery.

In the current study, we used three-dimensional computed tomographic bronchography and angiography (3D-CTBA) reconstruction to determine the patterns and variations of the bronchus and blood vessels of the superior segment of the right lower lobe (RS^6). The results were not directly compared to, but were discussed within the context of existing data as reported by Boyden (10) and Yamashita (11). We present this article in accordance with the STROBE reporting checklist (available at https://jtd.amegroups.com/article/view/10.21037/jtd-23-1607/rc).

Highlight box

Key findings

- Anatomical variations of the right S^6 segment are much more prevalent than previously reported.

What is known and what is new?

- The S^6 segmentectomy is classified as simple due to the single intersegmental plane between the superior and basal segments.
- In the current study, we used three-dimensional computed tomographic bronchography and angiography (3D-CTBA) reconstruction to determine the patterns and variations of the bronchus and blood vessels of the superior segment of the right lower lobe (RS^6). In our experience, surgical planning is extremely challenging without first performing a 3D reconstruction if the nodules are in close vicinity of V^6b or V^6c. We also observed several previously unreported variations (2 B^6 variations, 4 A^6 variations, and 5 V^6 variations).

What is the implication, and what should change now?

- The 3D-CTBA reconstruction should be performed pre-operatively to identify anatomic variations and thus avoid vascular damage and ensure complete resection of the tumor.

Methods

Clinical data and 3D-CTBA reconstruction

All the patients undergoing thoracoscopic segmentectomy for pulmonary nodules at the Thoracic Surgery Department of the First Affiliated Hospital of Nanjing Medical University between November 1, 2018 and March 28, 2021 were retrospectively enrolled in this study. Two-dimensional (2D) computed tomography (CT) images and three-dimensional (3D) reconstructed images were acquired to investigate the anatomical pattern of RS^6 bronchial arteries after 316 cases met the inclusion and exclusion criteria. Inclusion criteria: patients who underwent enhanced CT scans and 3D reconstruction. Exclusion criteria: (I) CT images were blurred and 3D-CTBA could not clearly show segmental branches of bronchi and vessels; (II) patients with prior history of lung surgery; (III) incomplete medical records. This study was conducted in accordance with the Declaration of Helsinki (as revised in 2013). This study was approved by the Ethics Review Committee of the First Affiliated Hospital of Nanjing Medical University (No. 2019-SR-123). Individual consent for this retrospective analysis was waived.

CT scan was performed using iopromide 370 (Uvixian;

Bayer Healthcare, Berlin, Germany) as the contrast agent with a Siemens first-generation dual-source CT (Somatom Definition; Siemens, Erlangen, Germany) in all patients. A 20–22 G venous indwelling needle was routinely inserted into the right anterior elbow vein. The patient was supine with head first. Firstly, the density time curve axis was obtained by the method of cluster injection test, and the start time of CT scan and the dosage of iodine contrast agent were set according to the curve axis. A time-density curve was first generated using a bolus test. Dosage of the contrast agent was calculated as follows: (peak time of ascending aorta − peak time of pulmonary artery + scan time) × 5. Delay time equaled the peak time of the ascending aorta. CT data were transferred to the DeepInsight software (Deepinsight, Oslo, Norway), a custom-built system developed by this group in collaboration with Neusoft Medical and Northeastern University (12). Data processing prior to 3D reconstruction of the bronchus and blood vessels included tracheal threshold calculation, tracheal extraction, blood vessel extraction, pulmonary nodule extraction, and adjustment of image window width and window position.

The surgical approach was categorized into three types, namely single subsegmentectomy, intrasegmental combined subsegmentectomy, and intersegmental combined subsegmentectomy, based on the nodular classification of subsegmental location. In the process of surgical simulation, a standard virtual margin of 2 cm was typically established for the nodule. However, if the nodule contained a higher proportion of solid components, the virtual margin would be proportionally increased. It is important to note that the virtual margin must not surpass the predetermined resection range; otherwise, an additional resection of adjacent subsegments becomes necessary (13).

Nomenclature

The terminology for the construction of the lung segments is based on Boyden's nomenclature for segmental bronchi and blood vessels (14), and included: B^6, segmental bronchus; B^6a, superior subsegmental bronchus; B^6b, lateral subsegmental bronchus; B^6c, medial subsegmental bronchus; A^6, segmental artery; A^6a, superior subsegmental artery; A^6b, lateral subsegmental artery; A^6c, medial subsegmental artery; V^6, segmental vein; V^6a1, intersubsegmental vein between S^6a and S^6c; V^6a2, intersubsegmental vein between S^6a and S^6b; V^6b1, intersegmental and intersubsegmental vein between S^6b and S^6c (V^6b1); V^6b2, intersegmental and intersubsegmental vein between S^6b and S^9a; V^6b3, intersegmental and intersubsegmental vein between S^6b and S^8a, and V^6c, intersegmental and intersubsegmental vein between S^6c and S^{10}a or S^7b.

Variation definition

The definition of variation is controversial in the existing literature (15). In this study, variations were defined as anatomical patterns that deviate from the normal anatomical location, co-stem origin, or normal return flow. The superior segment bronchus, vascular stems, and subsegmental bronchus of the right lower lobe, as well as the number of vascular bifurcations and the originating location, were used in this study to determine the anatomical pattern.

Statistical analysis

Statistical analysis was performed in SPSS (version 24). For descriptive analysis, the frequency (%) of the categorical variable was assessed. 3D-CTBA was drawn by Deepinsight method. The significance level was set at a two-sided P value below 0.05.

Results

The analysis included 316 patients (53.37±12.21 years of age; 209 women). The average maximum diameter of the nodules was 10.88±6.03 mm. The types of surgery included single pulmonary subsegmental resection (n=51; 16.1%), pulmonary segment combined with adjacent subsegmental resection (n=24; 7.6%), and single segment resections (n=161; 51.0%). Combined subsegmentectomy was conducted in 80 patients (25.3%). Postoperative complications occurred in 9 patients, and included pulmonary air leakage (n=8; treated successfully with infusion of 50 mL 50% glucose solution containing 1 g erythromycin into the pleural cavity) and hemoptysis (n=1; treated successfully with oral carbazochrome). Pulmonary infection, atelectasis, and pleural effusion were not observed.

The main planes included the leaf cleft plane, the rib plane, the spine plane, and the intersegmental plane. Small airways and vascular connections could be detected inside the leaf cleft as well as varying degrees of S^2 and S^6 fusion on the surface. The rib surface and the leaf cleft surface occasionally exhibited a false crack, typically between the

Table 1 Branching patterns of B^6

Branching patterns	Boyden (N=100), n (%)	Yamashita (N=180), n (%)	Our data (N=316), n (%)	P value*
B^6 arises as a single stem	94 (94.0)	180 (100.0)	305 (96.5)	0.267; 0.011
Bifurcates into				
B^6b and B^6a+c	79 (79.0)	112 (62.2)	178 (56.3)	<0.001; 0.2
B^6c and B^6a+b	4 (4.0)	11 (6.1)	52 (16.5)	0.003; 0.001
B^6a and B^6b+c	1 (1.0)	9 (5.0)	18 (5.7)	0.05; 0.084
Miscellaneous patterns	5 (5.0)	17 (9.4)	12 (3.8)	0.597; 0.01
Trifurcates into B^6a, B^6c and B^6b	5 (5.0)	22 (12.2)	45 (14.2)	0.013; 0.527
Quadrivial type	0	9 (5.0)	0	>0.99; <0.001
B^6 arises as two separate stems	6 (6.0)	0	11 (3.5)	0.267; 0.011
B^6b and B^6a+c	4 (4.0)	0	6 (1.9)	0.232; 0.063
B^6c and B^6a+b	0	0	1 (0.3)	0.573; 0.45
B^6a and B^6b+c	0	0	4 (1.3)	0.258; 0.13
Miscellaneous patterns	2 (2.0)	0	0	0.012; >0.99

*, P values indicate our data *vs.* Boyden and our data *vs.* Yamashita respectively.

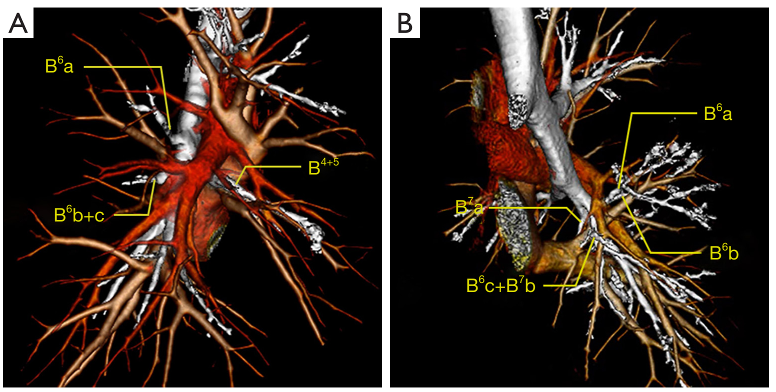

Figure 1 Anatomical variations of B^6. (A) B^6a arises independently from the intermediate bronchus (1.3%); (B) B^6c arises jointly with B^7b (0.3%).

superior segment and the basal segment. The position of the intersegmental plane between segments varied significantly.

B^6 had either a single (n=305, 96.5%) or 2 stems (n=11, 3.5%) (*Table 1*). For single-stem B^6, the patterns of bifurcations of the subsegmental bronchus included B^6a, B^6b+c (18/316, 5.7%), B^6b, B^6a+c (178/316, 56.3%), and B^6c, B^6a+b (52/316, 16.5%), as well as miscellaneous minor branches that crossed complementarily across subsegments (12/316, 3.8%). Trifurcation of the subsegmental bronchus (B^6a, B^6b, and B^6c) was seen in 14.2% (45/316) cases. The 2-stem B^6 included B^6b, B^6a+c (6/316, 1.9%); B^6c, B^6a+b (1/316, 0.3%) (B^6c and B^7b co-stem in 1 patient); B^6a, B^6b+c (B^6a alone above the right middle lobe bronchus, B^6b+c below the right middle lobe bronchus; 4/316, 1.3%). There were 2 types of B^6 variation (n=5; 1.6%). In 4 out of the 5 cases, B^6a originated from the intermediate bronchus alone, opposite to and slightly above the orifice of the middle lobe bronchus, and the orifice of B^6b+c was opposite and slightly below the orifice of the middle lobe bronchusorificeorificeorifice (*Figure 1A*). The remaining 1 case was B^6c and B^7b's co-trunk variation (*Figure 1B*).

The following branch patterns were observed for A^6

Table 2 Branching patterns of A^6

Branching patterns	Boyden (N=50), n (%)	Yamashita (N=130), n (%)	Our data (N=316), n (%)	P value*
A^6 arises as a single stem	40 (80.0)	103 (79.2)	188 (59.5)	0.005; <0.001
Bifurcates into				
A^6a+c and A^6b	25 (50.0)	17 (13.1)	65 (20.6)	<0.001; 0.063
A^6a+b and A^6c	4 (8.0)	10 (7.7)	20 (6.3)	0.657; 0.601
A^6b+c and A^6a	3 (6.0)	51 (39.2)	34 (10.8)	0.3; <0.001
Miscellaneous patterns	8 (16.0)	15 (11.5)	7 (2.2)	<0.001; <0.001
Trifurcates into A^6a, A^6c and A^6b	–	10 (7.7)	62 (19.6)	0.001; 0.002
A^6 arises as two separate stems	8 (16.0)	26 (20.0)	117 (37.0)	0.004; <0.001
A^6a+c and A^6b	–	19 (14.6)	74 (23.4)	<0.001; 0.038
A^6a+b and A^6c	–	7 (5.4)	29 (9.2)	0.026; 0.181
A^6b+c and A^6a	–	0	8 (2.5)	0.255; 0.067
Miscellaneous patterns	4 (8.0)	0	6 (1.9)	0.009; 0.114
A^6 arises as three separate stems	2 (4.0)	1 (0.8)	11 (3.5)	0.854; 0.108

*, P values indicate our data *vs.* Boyden and our data *vs.* Yamashita respectively.

Table 3 Anatomical variations of A^6

Anatomical variations	Number	Frequency, %
A^6 arising jointly with A^2	25	7.9
A^6b arising A^{9+10} or A^{10}	20	6.3
A^6c arising A^{9+10}	10	3.2
A^6 arising jointly with A^7	2	0.6
Total	57	18.0

(*Table 2*): (I) a single stem: (i) subsegmental artery bifurcates into: A^6a, A^6b+c (34/316, 10.8%); A^6b, A^6a+c (65/316, 20.6%); A^6c, A^6a+b (20/316, 6.3%); and miscellaneous (small branch cross-complementary between subsegments; 7/316, 2.2%); (ii) subsegmental artery trifurcates into: A^6a, A^6b, and A^6c (62/316, 19.6%); (II) 2 stems: A^6b, A^6a+c (74/316, 23.4%); A^6c, A^6a+b (29/316, 9.2%); A^6a, A^6b+c (8/316, 2.5%); and miscellaneous with a tiny branch that was cross-complementary across subsegments (6/316, 1.9%); (III) 3 stems: A^6a, A^6b, and A^6c (11/316,3.5%); and a miscellaneous (identification is challenging due to the short cross-complementary branching between subsegments; 2/316, 0.6%).

A^6 variations included (*Table 3*) the following: (I) coexistence of A^6 and A^2 (n=25, 7.9%; *Figure 2A*); (II) A^6b originating from A^{9+10}/A^{10} alone (n=20, 6.3%); (III) A^6c originating from A^{9+10} (n=10, 3.2%; *Figure 2B*); (IV) co-draining of A^6 and A^7 (n=2, 0.6%; *Figure 2C*).

The segments and sub-segments of V^6 and its branches did not seem to be related to either B^6 or A^6 and its branches. The backflow patterns of V^6 included (*Table 4*) the following: (I) a single stem: (i) subsegmental vein bifurcates into: V^6a, V^6b+c (68/316, 21.5%); V^6b, V^6a+c (44/316, 13.9%); and V^6c, V^6a+b (92/316, 29.1%); (ii) the subsegmental vein trifurcates into: V^6a, V^6b, and V^6c (94/316, 29.7%); (II) 2 stems: V^6a, V^6b+c (5/316, 1.6%); V^6c, V^6a+b [n=12 for V^6c backflow to the basal segment vein (3.8%); n=1 for V^6c backflow to V^{10}].

V^6 variations included (*Table 5*) the following: (I) co-draining of V^6 and V^2 (n=20, 6.3%; *Figure 3A*); (II) co-draining of V^6 and V^4 (n=5, 1.6%); (III) V^6 and V^{8+9} co-draining (n=3, 0.9%); (IV) V^6 draining into the superior pulmonary vein (n=4, 1.3%; *Figure 3B*); and (V) direct V^6 draining into the left atrium (n=5, 1.6%; *Figure 3C*).

Discussion

Segmentectomy was first reported in 1972 by Bonfils-Roberts and Clagett (16) as a treatment option for lung cancer patients who are elderly and have poor cardiopulmonary function. Subsequent research by Jensik

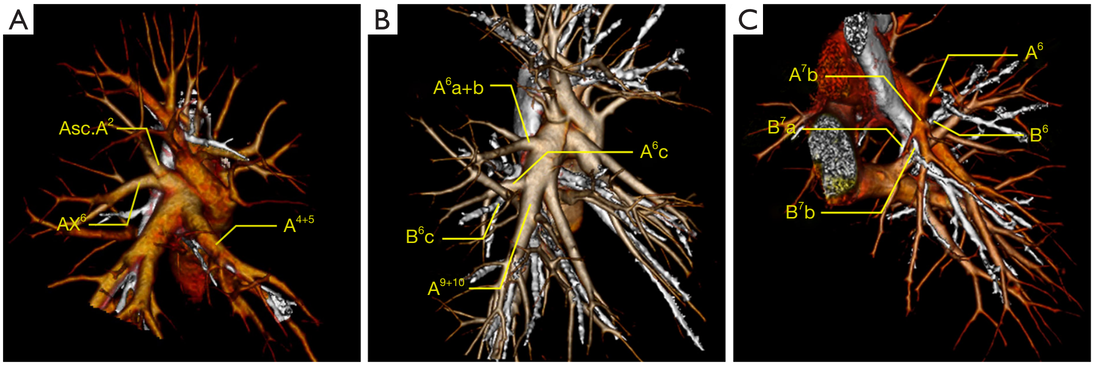

Figure 2 Anatomical variations of A^6. (A) A^6 arises jointly with A^2 (7.9%); (B) A^6c arises from A^{9+10} (3.2%); (C) A^6 arises jointly with A^7 (0.6%). According to the bronchial and blood vessel nomenclature described by Boyden in 1946, the letter "X" first appeared, and the structure derived from adjacent lung segments or subsegments in the position of normal lung segments or subsegments was named "X", indicating abnormal co-trunk.

Table 4 Branching patterns of V^6

Branching patterns	Yamashita (N=130), n (%)	Our data (N=316), n (%)	P value
V^6 converges as a single stem	110 (84.6)	298 (94.3)	0.001
Formed by two branches	91 (70.0)	204 (64.6)	0.270
V^6a+c and V^6b	24 (18.5)	44 (13.9)	0.226
V^6a+b and V^6c	19 (14.6)	92 (29.1)	0.001
V^6b+c and V^6a	20 (15.4)	68 (21.5)	0.139
Miscellaneous patterns	28 (21.5)	0	<0.001
Formed by V^6a, V^6c and V^6b	19 (14.6)	94 (29.7)	0.001
V^6 converges as two separate stems	20 (15.4)	18 (5.7)	0.001
V^6c from V^{10}	9 (6.9)	1 (0.3)	<0.001
V^6c from CBV	8 (6.2)	12 (3.8)	0.275
V^6b+c and V^6a	0	5 (1.6)	0.149
Miscellaneous patterns	3 (2.3)	0	0.007

CBV, common basal vein.

Table 5 Anatomical variations of V^6

Anatomical variations	Number	Frequency, %
V^6 + V^2	20	6.3
V^6 + V^4	5	1.6
V^6 + V^{8+9}	3	0.9
V^6 drains into SPV	4	1.3
V^6 drains into left atrium	5	1.6
Total	37	11.7

SPV, superior pulmonary vein.

et al. (17) reported comparable oncological efficacy of segmentectomy versus lobectomy for early-stage lung cancer. Since then, segmentectomy has been increasingly used in patients with early-stage lung cancer. The benefits of segmentectomy in the treatment of peripheral non-small cell lung cancer with diameter 2 cm and with pathologically confirmed no nodal disease by 2 important trials: the Japanese Clinical Oncology Organization JCOG0802/WJOG4607L trial and CALGB study (2,3). However, there have been few studies on the morphological patterns and variant types of segmental bronchi, arteries, and veins,

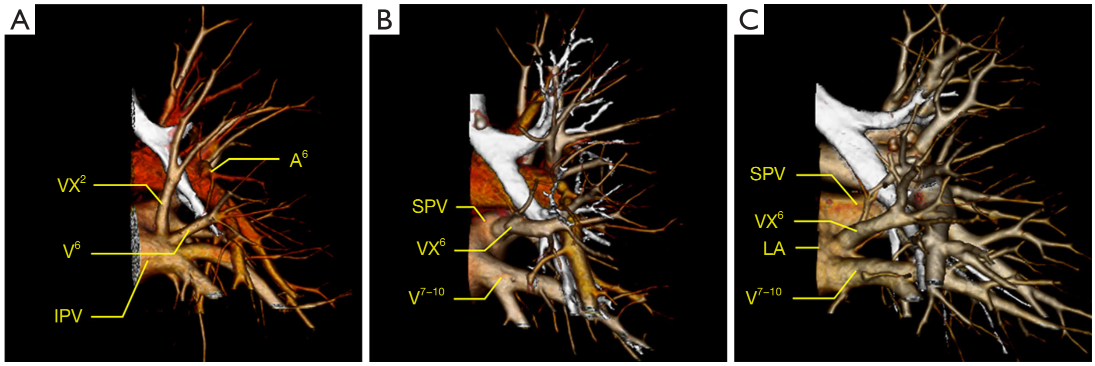

Figure 3 Anatomical variations of V^6. (A) The common trunk of right V^6 and V^2 flows into the inferior pulmonary vein (6.3%); (B) V^6 drains into the superior pulmonary vein (1.3%); (C) V^6 draining into the left atrium (1.6%). According to the bronchial and blood vessel nomenclature described by Boyden in 1946, the letter "X" first appeared, and the structure derived from adjacent lung segments or subsegments in the position of normal lung segments or subsegments was named "X", indicating abnormal co-trunk. IPV, inferior pulmonary vein; SPV, superior pulmonary vein; LA, left atrium.

with autopsy studies of limited sample size (18,19) and case reports (20). The use of 3D CT bronchial vascular reconstruction technology has now replaced traditional anatomical studies to examine the variation of the bronchi, pulmonary arteries, and veins (21).

The results from the current study showed that the dominant pattern of the bronchus B^6 was single-stem bifurcated 2 branches type (260/316, 82.3%). Under this pattern, the superior subsegment and medial subsegment bronchus co-trunk (B^6a+c) was seen in 56.3% of the cases. B^6 variation was infrequent. In 4 patients (1.3%), B^6a originated from the intermediate bronchus alone, with the orifice above the middle lobe bronchus orifice, and B^6b+c opened below the middle lobe bronchus orifice. According to this finding, B^6a and B^6b+c should be treated individually during right superior segmentectomy to prevent unintentional damage to the right middle lung bronchus, stenosis of the right middle lung bronchus, and omission of B^6b+c and thus insufficient resection margin. Another rare variation (n=1) is the co-trunk of B^6c and B^7b, and the genesis of B^6a+b from the intermediate bronchus. Although rare, caution must be exercised to prevent damaging the B^7b co-trunk with B^6c.

We identified a total of 11 A^6 patterns. Consistent with a previous study (22), the most common patterns in the current study included single-stem bifurcation (39.9%) and single-stem trifurcation (19.6%). Notably, 2- and 3-stem patterns (A^6a, A^6b, or A^6c from the interlobar trunk or as an A^9/A^{9+10} alone) were more common than previously reported by Yamashita (20.0% and 0.8%, respectively) (11). Co-stem with A^2 was the most frequent variation form of A^6 (n=25, 7.9%). Patients who had hypoplasia of the posterior oblique fissure frequently displayed this anomaly. When performing right upper lobectomy or posterior segmentectomy of the right upper lobe, caution should be taken to prevent inaccurate resection of A^6. Similarly, attention should be taken when performing right lower pulmonary segmentectomy or right lower lobectomy to avoid inaccurate resection of A^2. These patterns highlight the importance of preoperative planning based on CT or 3D-CTBA to achieve safe separation of the oblique fissure between the upper and lower lobes in segmentectomy.

V^6 was classified into 7 patterns in the current study, and consistent with the Yamashita report, single-stem bifurcation was the most common pattern (64.6%). V^6c, V^6a+b accounted for 29.1% of the cases; V^6a, V^6b+c accounted for 21.5% of the cases; and V^6b, V^6a+c accounted for 13.9% of the cases. It is important to note that the intersegmental plane was defined by V^6c between S^6 and S^{10}. When V^6c originated from the common basal vein or V^{10} alone, the superior segment tended to occupy more space of the lower lobe. Such individual variations must be taken into consideration when clipping the intersegmental plane contact between the superior segment and the basal segment to ensure adequate resection margins. The most frequent V^6 variation was V^6/V^2 co-trunk (n=20; 6.3%). When performing S^6 or right lower lobectomy and S^2 or right upper lobectomy, caution must be exercised to avoid severing the trunk.

In a previous 3D image study of 20 patients undergoing

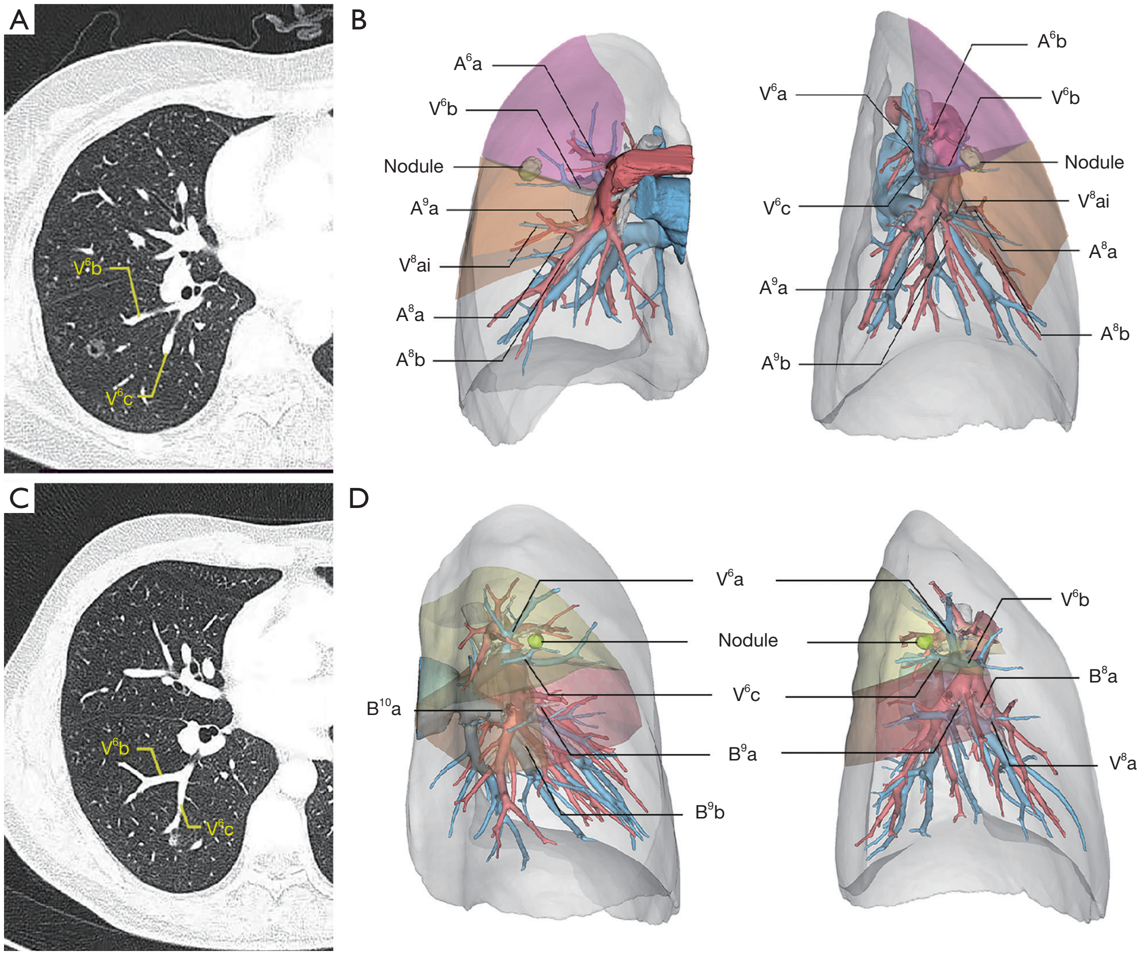

Figure 4 Intersegmental combined subsegmentectomy for nodules close to V^6b and V^6c. (A,B) The nodule was close to V^6b. Segmentectomy would result in insufficient surgical margins. S^6b+S^8a combined subsegmentectomy is conducive to adequate surgical margins. (C,D) The nodule was close to V^6c. S^6c+S^9a+S^{10}a combined subsegmentectomy was preferred.

thoracoscopic segmentectomy by Nakao *et al.* (23), the 3D images were rated as "good" in terms of anatomical validity in 19 (95%) patients and as "good" in terms of anatomical consistency in 18 (90%) patients. Clearly, preoperative assessment based on CT and 3D-CTBA images is helpful to comprehend the relevant anatomical patterns and variations in patients undergoing segmentectomy and subsegmentectomy (24,25). The results in the current study differed significantly from that by either Boyden or Yamashita. Such a discrepancy could be partly attributed to the use of specialized imaging methods and 3D reconstruction in the current study, which in turn allowed us to obtain results that were as close to actual lung ventilation as possible.

Patients undergoing superior segmentectomy for early-stage lung cancer tend to have worse long-term oncological outcomes than segmentectomy at other locations. Nakazawa *et al.* attributed this phenomenon to clipping the intersegmental plane. We concur with Nakazawa's assertion that the right lower lobe superior segmentectomy's subpar results were likely caused by insufficient surgical margins (9). In our experience, surgical planning is extremely challenging without first performing a 3D reconstruction if the nodules are in close vicinity of V^6b or V^6c. V^6b lies between S^6b, S^8a, and S^9 (26). Accordingly, resection of RS^6 alone tends to result in insufficient resection margins for nodules close to V^6b (*Figure 4A,4B*). For such cases, we previously proposed sublobar resection based on subsegment plan (27). Based on the results of the current study, we now believe that the best treatment for such cases is intersegmental combined subsegmentectomy, for example, S^6/S^6b+S^8a or S^6/S^6b+S^8a+S^9a resection. Similarly, for lesions in the vicinity of V^6c (*Figure 4C,4D*), we recommend S^6/S^6c+S^{10}/subsuperior segment/or S^7b resection.

The current study has several limitations. First, the data were based on patients at a single center with homogeneous ethnicity, mainly aimed at the Chinese population. Such results may be related to selection bias caused by the small sample size we selected. Whether the findings are generalizable to other populations is unknown. Second, minor branches (for example, <2 mm in diameter) may not be visible in 3D-CTBA, but could be functionally important. Third, to what extent the information obtained from the current study could improve surgical planning requires further studies.

Conclusions

Variation of segmental blood vessels, particularly the arteries and veins, in RS^6 is much more common than previously thought. We also observed several previously unreported variations (2 B^6 variations, 4 A^6 variations, and 5 V^6 variations). In particular, when the nodule is close to the V^6b or V^6c, surgical planning based on 3D reconstruction could be useful.

Acknowledgments

Funding: None.

Footnote

Reporting Checklist: The authors have completed the STROBE reporting checklist. Available at https://jtd.amegroups.com/article/view/10.21037/jtd-23-1607/rc

Data Sharing Statement: Available at https://jtd.amegroups.com/article/view/10.21037/jtd-23-1607/dss

Peer Review File: Available at https://jtd.amegroups.com/article/view/10.21037/jtd-23-1607/prf

Conflicts of Interest: All authors have completed the ICMJE uniform disclosure form (available at https://jtd.amegroups.com/article/view/10.21037/jtd-23-1607/coif). A.B. reports that he is the member of advisory board and recipient of speaker honoraria with Astra Zeneca, BMS, MSD, Ethicon and Roche, and Director of the Board of the ESTS and STS. The other authors have no conflicts of interest to declare.

Ethical Statement: The authors are accountable for all aspects of the work in ensuring that questions related to the accuracy or integrity of any part of the work are appropriately investigated and resolved. This study was conducted in accordance with the Declaration of Helsinki (as revised in 2013). This study was approved by the Ethics Review Committee of the First Affiliated Hospital of Nanjing Medical University (No.2019-SR-123). Individual consent for this retrospective analysis was waived.

References

1. Suzuki K, Watanabe SI, Wakabayashi M, et al. A single-arm study of sublobar resection for ground-glass opacity dominant peripheral lung cancer. J Thorac Cardiovasc Surg 2022;163:289-301.e2.
2. Altorki N, Wang X, Kozono D, et al. Lobar or Sublobar Resection for Peripheral Stage IA Non-Small-Cell Lung Cancer. N Engl J Med 2023;388:489-98.
3. Saji H, Okada M, Tsuboi M, et al. Segmentectomy versus lobectomy in small-sized peripheral non-small-cell lung cancer (JCOG0802/WJOG4607L): a multicentre, open-label, phase 3, randomised, controlled, non-inferiority trial. Lancet 2022;399:1607-17.
4. White A, Swanson SJ. Video-assisted thoracic surgery (VATS) segmentectomy: state of the art. Minerva Chir 2016;71:61-6.
5. Handa Y, Tsutani Y, Mimae T, et al. Surgical Outcomes of Complex Versus Simple Segmentectomy for Stage I Non-Small Cell Lung Cancer. Ann Thorac Surg 2019;107:1032-9.
6. Jones GD, Caso R, Choe G, et al. Intentional Segmentectomy for Clinical T1 N0 Non-small Cell Lung Cancer: Survival Differs by Segment. Ann Thorac Surg 2021;111:1028-35.

7. Handa Y, Tsutani Y, Tsubokawa N, et al. Clinical Prognosis of Superior Versus Basal Segment Stage I Non-Small Cell Lung Cancer. Ann Thorac Surg 2017;104:1896-901.
8. Watanabe S, Suzuki K, Asamura H. Superior and basal segment lung cancers in the lower lobe have different lymph node metastatic pathways and prognosis. Ann Thorac Surg 2008;85:1026-31.
9. Nakazawa S, Yajima T, Shirabe K. Superior S(6) Segment, a Wolf in Sheep's Clothing? Ann Thorac Surg 2021;112:686-7.
10. Boyden EA. Segmental anatomy of the lung. New York: McGraw-Hill; 1954.
11. Yamashita H. Roentgenologic anatomy of the lung. New York: Igaku-Shoin Medical Publishers; 1978.
12. Zhang W, Chen L, Wang J, et al. A Study on the Authenticity of Preoperative Pulmonary Bronchial Angiography by DeepInsight Software. Zhongguo Fei Ai Za Zhi 2021;24:88-93.
13. Chen L, Zhu Q, Wu W, et al. Atlas of thoracoscopic anatomical pulmonary subsegmentectomy. Amsterdam: Elsevier; 2023.
14. Boyden EA. The intrahilar and related segmental anatomy of the lung. Surgery 1945;18:706-31.
15. Fan K, Feng JT, Wang HY, et al. Anatomy of upper lung lobes of patients with small pulmonary nodules based on three-dimensional reconstruction of PC. Chinese Journal of Thoracic and Cardiovascular Surgery 2020;36:557-61.
16. Bonfils-Roberts EA, Clagett OT. Contemporary indications for pulmonary segmental resections. J Thorac Cardiovasc Surg 1972;63:433-8.
17. Jensik RJ, Faber LP, Kittle CF. Segmental resection for bronchogenic carcinoma. Ann Thorac Surg 1979;28:475-83.
18. FERRY RM Jr, BOYDEN EA. Variations in the bronchovascular patterns of the right lower lobe of fifty lungs. J Thorac Surg 1951;22:188-201.
19. Jiang JY. Surgical anatomy of bronchopulmonary segment. Shanghai: Shanghai Scientific & Technical Publishers; 1960;22-5.
20. Akiba T, Marushima H, Kamiya N, et al. Thoracoscopic lobectomy for treating cancer in a patient with an unusual vein anomaly. Ann Thorac Cardiovasc Surg 2011;17:501-3.
21. Yoldas B, Gursoy S. A pulmonary vascular variation to be considered in resective lung surgical procedures. Ann Thorac Surg 2014;97:715.
22. Nagashima T, Shimizu K, Ohtaki Y, et al. Analysis of variation in bronchovascular pattern of the right middle and lower lobes of the lung using three-dimensional CT angiography and bronchography. Gen Thorac Cardiovasc Surg 2017;65:343-9.
23. Nakao M, Omura K, Hashimoto K, et al. Novel three-dimensional image simulation for lung segmentectomy developed with surgeons' perspective. Gen Thorac Cardiovasc Surg 2021;69:1360-5.
24. Akiba T, Marushima H, Harada J, et al. Anomalous pulmonary vein detected using three-dimensional computed tomography in a patient with lung cancer undergoing thoracoscopic lobectomy. Gen Thorac Cardiovasc Surg 2008;56:413-6.
25. Yamada S, Suga A, Inoue Y, et al. Importance of preoperative assessment of pulmonary venous anomaly for safe video-assisted lobectomy. Interact Cardiovasc Thorac Surg 2010;10:851-4.
26. Chen L, Zhu Q, Wu W, et al. Atlas of thoracoscopic anatomical pulmonary subsegmentectomy (Chinese). Nanjing: Southeast University Press; 2021.
27. Wu W, He Z, Xu J, et al. Anatomical Pulmonary Sublobar Resection Based on Subsegment. Ann Thorac Surg 2021;111:e447-50.

Cite this article as: Zhu S, Xu W, Li Z, Wu W, Brunelli A, Matsuura Y, Maurizi G, Tosi D, Bouabdallah I, Gossot D, Chen L. Branching patterns and variations of the bronchus and blood vessels in the superior segment of the right lower lobe: a three-dimensional computed tomographic bronchography and angiography study. J Thorac Dis 2023;15(12):6879-6888. doi: 10.21037/jtd-23-1607

